ORIGINAL SCIENTIFIC PAPER

CROATICA CHEMICA ACTA

Croat. Chem. Acta **2020**, *93*(4), 349–365
Published online: December 22, 2021
DOI: 10.5562/cca3790

HKD 1926

"Pure-Polyhex" π-Networks: Topo-Combinatorics

Douglas J. Klein,[1,*] Bholanath Mandal[2]

[1] Department of Foundational Sciences, Texas A&M University at Galveston, TX 77553, USA
[2] Department of Chemistry, The University of Burdwan, Burdwan-713104, India
* Corresponding author's e-mail address: kleind@tamug.edu

RECEIVED: May 20, 2021 * REVISED: August 16, 2021 * ACCEPTED: August 18, 2021

— THIS PAPER IS DEDICATED TO PROF. MILAN RANDIĆ ON THE OCCASION OF HIS 90TH BIRTHDAY, AND TO THE MEMORY OF PROF. MIRCEA DIUDEA —

Abstract: Structural possibilities are considered for what arguably is the most general class of connected "pure-polyhex" π-networks (of carbon atoms). These are viewed as hexagonal-network coverings (*i.e.*, a tiling by hexagons) of a connected locally Euclidean surface *S* possibly with holes which can be simple cycles of sizes other than 6. The surface *S* can curve around to connect to itself in different ways, *e.g.*, with handles of different sorts. This then includes ordinary benzenoids, coronoids, carbon nanotubes, bucky-tori, carbon nano-cones, carbon nano-belts, certain fullerenes & fulleroids, various benzenoid polymers, a great diversity of defected (disclinational or dislocational) graphene flakes, and many other novel pure-polyhexes. A topological classification is made, and several combinatorial conditions on chemical sub-structure counts are identified. These counts include that of "combinatorial curvature", such as is related to curvature stresses, as also relate to the Gaussian curvatures of the embedding surface.

Keywords: pure-polyhex networks, surface decorations, hexagonal coverings, Euler-Poincaré characteristics, Gaussian and combinatorial curvatures.

INTRODUCTION

CONJUGATED π-networks have been much studied, since from before the time of Kekulé, with recent intense excitement upon the discovery of fullerenes, of carbon nano-tubes, and of grapheneic structures. For the purpose of constructing nano-devices much interest has developed in additional novel structures: decorated nano-tubes, branched nano-tubes, carbon nano-belts, bucky-cones, negatively curved structures, and more. Typically these species may be viewed as conjugated π-networks based upon a polyhex-tiled surface with various defect rings of other sizes punched in the surface. The classical benzenoids can be considered as polyhex species covering a surface topologically equivalent to a disk. Coronoids are pure-polyhex species tiling a surface topologically equivalent to a punctured disk. The carbon nano-tubes (or bucky-tubes) are purely polyhex in the bulk of the surface which appears like a long cylinder, while something also occurs at the ends, such as an opening at each end (to make the surface overall topologically equivalent to an open-ended cylinder, or equivalently again to a punctured disk). If both ends are suitably closed off, a fullerene again can be obtained, though there are other possibilities with smaller sized rings, especially if the smaller sized rings abutt to one another – in which case a "fulleroid" may result. But there are many more possibilities for polyhex-covered surfaces – both finite & infinite.

The implications on substructural counts (say of atoms, edges, rings, & boundary features) have already been studied for several special cases. Gutman[1] & others[2–5] have emphasized such combinatoric aspects for the particular case of a pure polyhex with a surface topologically equivalent to a disk, with Dias exhibiting[2,3] results in terms of a "formula periodic table of benzenoids". And further there have been comparable studies of what occurs when one[6,7] or a few[8–17] other-size rings are allowed, all focused on the circumstance of a planar network with otherwise a single outer boundary. The case of coronoids (as benzenoids with a hole) also has been similarly studied, as well as multi-coronoids (albeit to a lesser extent) – reviewed in Ref. [18] The case of fullerenes

is also extensively studied, [19–21] with the count of 12 pentagons being very well known. Harris[22] and Sadoc & Mosseri[23,24] have generally discussed polygon-tiled surfaces topologically equivalent to a sphere, with attention to the relation to Gaussian curvature – with "curvature" effects in fullerenes have also been relevant.[25,26] The circumstance of covering a torus has been considered quite separately, either purely[27–29] with hexagons, or with a few other-sized rings[30,31] mixed in to (partially) relieve stress. There are many works concerning Möbius arrangements involving a Möbius strip defined to contain all the π-orbital axes (instead of our strips containing all the conjugated-carbon *σ*-network) – this alternative starts with Heilbronner[32]). As to infinite structures, the hexagon-tiled nanotubes have been (comprehensively) addressed,[33] and then there is graphene & substructures cut from it, as well as its vacancy defects.[34]

Here we pursue a general comprehensive investigation of possible surfaces and commensurate polyhex *π*-network structures thereon. That is, rather arbitrary topologies are allowed for the connected surface to be exactly covered by hexagons in a suitable fashion: every edge of the network is in either 1 or 2 hexagons, and every site is of degree 3 or 2. Upon covering by hexagons, the surface is said to be hexagonally *tiled*. Some modest degree of standard topology is used – *e.g.*, as in[35–38] use is made of *homeomorphism* which is a mapping of one geometrical set to another through continuous neighborhood-preserving transformation. Thus benzenoids are viewed as: polyhexes on a (topological) "disk"; coronoids (& multi-coronoids), on punctured (& multi-punctured) "disks"; "poly-*q*-polyhexes"[6–13] (with nonadjacent *q*-gons) also as punctured "disks" (with punctures corresponding to non-hexagonal rings); tori, with or without punctures; polyhex bracelets (which are not coronoids or multi-coronoids, including both untwisted & Möbius possibilities); many extended (*i.e.* infinite) benzenoid or coronoid polymers; bucky-tubes; fullerenes (with isolated pentagons); high-genus negatively curved graphene surfaces[39,40] (with punctures for non-hexagonal rings); disclinationally or dislocationally defected[41] graphenes; *etc*. A collection of chemically oriented contributions (without restriction to conjugated-carbon networks) is found in Sauvage *et al*'s monograph.[42] Here a major aim is to identify a collection of theorems and combinatorial results for different substructure counts – often very well-known for classical benzenoids, but here seeking wider limits and modifications to their applicability. Ultimately the topo-combinatorics relates to geometric curvatures, complicit stresses, & realizable embeddings into ordinary space. Further the diverse topological possibilities for polyhex tilings of surfaces are indicated.

Theoretical investigators Ed Kirby, Ivan Gutman, Sven Cyvin, J. R. Dias, Milan Randić, Nenad Trinajstić, M. Terrones, A. T. Balaban, M. Diudea, P. W. Fowler, and many more have already explored various polyhex conjugated-carbon π-networks.

FUNDAMENTALS & INITIAL STRUCTURES

Here a *π*-network is viewed as a graph *G*, with any H atoms bonded to any of the carbon atoms deleted from this otherwise carbon network. The pairs of *σ*-bonded *π*-centers in the *π*-network are identified to edges of *G*. The restriction to trigonal (sp^2) *π*-centers limits the degree of each site to no more than 3. The whole network *G* is imagined to be "suitably" embedded in a connected smooth surface *S*, which in turn is embedded in 3-dimensional Euclidean space $\mathcal{E}_3$. Any boundaries of *S* correspond to edges (*i.e.*, bonds) of *G*, and "rings" of *G* bound (near-planar) disk-like regions (faces) of *S*. The surface *S* is to be *locally Euclidean* in that its points have open sets (of *S*) homeomorphic either to an open disk or to a boundary point as for a point of a disk. The graph *G* is to be embedded in *S* and to consist entirely of hexagons exactly covering *S*, such that every edge of *G* occurs in exactly 1 or 2 hexagons. That the associated surface *S* is to be a conjugated whole precludes three surfaces meeting at a seam (because conjugation entails at least approximately a mutual alignment of *π*-orbitals and this in turn implicates a smoothly varying normal to *S*, as would not occur at a seam). Moreover, the hexagons are typically imagined to be of comparable sizes, and the surface not to fluctuate notably below or even at the scale of the size of these faces. That is, radii of linear curvature of the surfaces are to be a somewhat greater than the bond lengths, and areas of faces on *S* are to be not too different from that for a regular polygon with edges of lengths similar to that of the faces. A boundary of the network (and of *S*) is identified such that every degree-2 vertex of *G* appears on the boundary, along with the edges (bonds) incident to these sites. Generally some vertices of degree 3 may be identified to the boundary – when there are 2 boundary edges incident thereto. See, *e.g.*, the "coronoid-like" structure of Figure 1. That is, the surface is *tiled* by hexagons with no more than 3 hexagons meeting at any vertex, such that it takes exactly 3 to completely surround a vertex, whence such a graphical structure is termed a *pure polyhex*. These structures do not account for all conjugated *π*-networks – but it does recognize the propensity for hexagonal rings so as to encompass a large variety of possibilities, many of which are realized, and many more as yet unrealized. Besides benzenoids, it allows bucky-cones, bucky-tori, diverse defected grapheneic flakes, and more. It allows isolated-

pentagon-rule fullerenes as 12-fold punctured spheres – and it allows "fulleroids" with isolated rings of other sizes. This is a considerably more general than the usual definition of a polyhex π-network (of sp^2 carbons), so that questions naturally arise as to how different earlier results for more limited structures might generalize.

Some initial considerations are appropriate for a finite *benzenoid B* (=*G*), which is taken to be a region of the Euclidean plane homeomorphic to a disk and fully tiled by hexagonal faces (or rings). Often the hexagonal rings are required to be geometrically regular, in which case the benzenoid is a part of the honeycomb lattice net. A *coronoid C* (=*G*) is viewed as a benzenoid with a hole cut out of the center, such that the remaining region of *S* is fully tiled by hexagons, which again are often required to be geometrically regular. See Figure 1. If two or more holes are cut from a benzenoid then a *multi-coronoid* results, still with every edge in a hexagonal face.

For a single (benzenoid) boundary δ, procession (say) clockwise around δ (with the bulk of *B* on the right), gives a number of right turns & a number of left turns, with the excess of right turns over left turns being +6 to accomplish a full cycling of $6 \times (\pi / 3) = 2\pi$ radians. Also note that each right turn corresponds to a degree-2 C atom, with an attached H atom, whereas each left turn (if any) corresponds to a degree-3 C atom, with no H atom. See Figure 1.

It might seem that the preceding argument depends on the regularity of the hexagonal faces, but its essence does not. To see this, consider the "helicenic" example *B* of Figure 2, and imagine *B* to be the result of 2 (potentially) regular-faced benzenoids B_1 & B_2 fused together at their bold-faced edges (as indicated in Figure 2). The clockwise-oriented circuits C_1 & C_2 around B_1 & B_2 each entail a total turn through an excess of 6 right 60° -turns over left turns. Furthermore the clockwise boundary circuit of *B* can be viewed as a "sum" of C_1 & C_2, where the common (oppositely oriented) edge is canceled, and the 4 right (60°) turns (of C_1 & C_2 at this edge) are traded for 2 left turns. Thus the total excess of right turns over left turns around *C* remains 6. Of course, even for the deformed *B* in Figure 2 there is a net turn of $360^\circ = 2\pi$rad as one traverses the circuit (even though the hexagons are deformed). Note each right turn entails a degree-2 site, while each left turn entails a degree-3 site, allows a boundary correspondence amongst: net turning angle; excesses of degree-2 over degree-3 sites; and numbers of H atoms versus total boundary length. Such structures are here termed *generalized benzenoids*. The differences for the numbers of left & right turns still turns out to be 6 (even if the angles are not precisely 60° turns as in the first part of Figure 2.

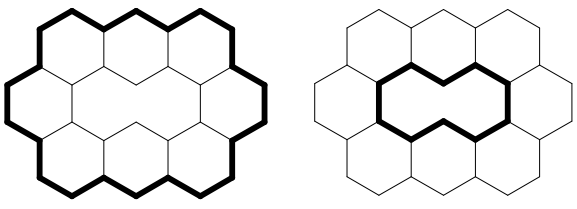

Figure 1. A polyhex structure which if the missing central bond were there, would be a (regular) benzenoid. With the hole in the middle, it is a (regular) coronoid. On the left the outer boundary is in bold-face, while on the right the inner boundary is in bold-face.

For a coronoid, the turns around the inside boundary δ_{in} still satisfy a condition: procession with the near part of *S* on the right now means a counter-clockwise circuit with the number of left turns exceeding the number of right turns by +6. Again the right turns correspond to vertices of degree 2 while the left turns correspond to vertices of degree 3. Again see Figure 1.

The noted results extend fairly straight-forwardly to a multi-coronoid *M* (=*G*), which may be viewed as obtained from a benzenoid by deleting several regions to leave several holes, each made by deletion of ≥ 2 hexagons, while still requiring the remnant region to be fully tiled by hexagons. If the hexagons are geometrically regular, similar results apply. These results are conveniently made independent of the direction of cycling about a boundary circuit δ, if they are expressed in terms of the numbers $n_{2,M}(\delta)$ of degree-2 vertices & $n_{3,M}(\delta)$ of degree-3 vertices on δ (with the degrees measured in *M*), as well as the number $n_{holes}(M)$ and the total number $n(\partial M)$ of boundary sites. Now:

Theorem 1 – Let *M* be a finite generalized benzenoid, coronoid, or multi-coronoid. Then for any cyclic boundary δ of *M*,

$$n_{2,M}(\delta) - n_{3,M}(\delta) = \pm 6 \,,$$

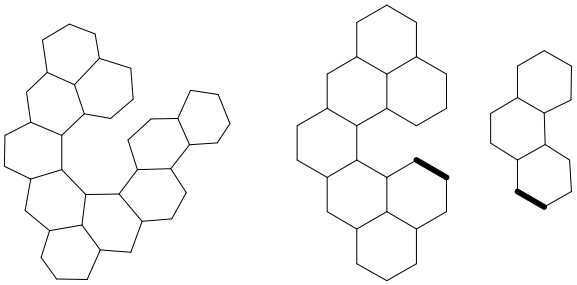

Figure 2. A benzenoid *B* unable to be embedded in $\mathcal{E}_2$ with regular hexagonal faces, and its decomposition into B_1 & B_2 each of which is representable with regular hexagonal faces. (In chemical reality, *B* would not remain in C_2, but rather the part B_2 would deviate out of the plane so that it lays above (or below) the earlier part, while maintaining rings which are more nearly regular hexagons.)

with the + sign applying for the outer boundary, and the – sign applying for any inner boundary. The number of H atoms in M is

$$n_{\mathrm{H}}(M) = \sum_{\delta}^{M} n_{2,M}(\delta) = \{n(\partial M) + 6 - 6n_{\mathrm{holes}}(M)\} / 2 \, .$$

Proof: Most of the proof is already done, excepting the last relation for the number of H atoms. Here for the outer boundary $\delta = \delta_{\mathrm{out}}$, $n(\delta) = n_{2,M}(\delta) + n_{3,M}(\delta)$ & $n_{3,M}(\delta) - n_{2,M}(\delta) = 6$, so that the number of H atoms on this outer boundary is $n_{\mathrm{H}}(\delta) = \{n(\delta) + 6\} / 2$. And much the same argument gives the number of H atoms on an inner boundary $\delta = \delta_{\mathrm{in}}$ as $n_{\mathrm{H}}(\delta) = \{n(\delta) - 6\} / 2$. Summing over all the cyclic boundaries δ, and noting that there is a number $n_{\mathrm{holes}}(M)$ of such inner boundaries, finally leads to the given result. ■

This result (for benzenoids) is known – as in,[2–4,18] where in fact there are some further enumerative relations, which are here addressed later (in a generalized form). The statement of this theorem does not mention the relation to angular turns, but this lack mirrors these earlier references, and here we return to the turn-angle aspect in a more general context. This theorem provides a first example of the sort of combinatorial information here considered – and it also provides a fundamental reference circumstance for the more general structures G contemplated.

Let us note something concerning embeddings, in $\mathcal{E}_2$. The benzenoid B (coronene) in the first part of Figure 3 may be embedded in a second fashion as in the second part of this figure. We use a convention that given any hexagonal ring, the part of the empty part of this hex region is to be identified as part of our embedding surface, with the area of this hexagon surface finite. Thus in the last part of Figure 3, the region containing the dashed line is to be part of the "outer" surface hexagon, but should be finite – so that the drawing of the first part of Figure 3 is correct. (If instead we imagine the second drawing to occur on the surface of a (big) sphere, then this outside part of the surface is finite, and the result is the same as dealing with the standard coronene drawing in the first part of our figure.

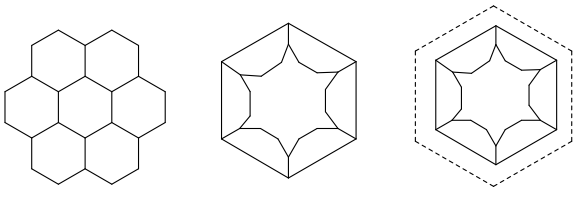

Figure 3. First a benzenoid structure, then second another embedding in a non-canonical way. Third a dashed line to be part of the embedding surface for G.

FUNDAMENTAL "EULEROLOGY"

For our graph embeddings, a surface S is topologically characterized in terms of its *Euler* (or Euler-Poincaré) *characteristic* $\chi(S)$. Indeed a quite general compact set[43,44] S in $\mathcal{E}_n$ manifests such a characteristic $\chi(S)$ invariant under homeomorphic transformations of S. This general Euler-Poincaré characteristic has the value 0 for the empty set, the value 1 for a point, and satisfies

$$\chi(R) + \chi(T) = \chi(R \cup T) + \chi(R \cap T) \qquad (1)$$

Indeed this allows the (easy) determinations for rather general (compact & topologically closed) geometric sets R & T – *e.g.*, as emphasized by Hadwiger[42,43] and others.[26,45,46] Indeed one has:

Lemma 2 – Values of the Euler characteristic of several compact geometric sets S are:
$S =$ circle, open-ended cylinder, Möbius strip, punctured disk, or torus $\Rightarrow \chi(S) = 0$
$S =$ line segment or disk $\Rightarrow \chi(S) = 1$
$S =$ sphere $\Rightarrow \chi(S) = 2$

Proof: First, if two line segments L_1 & L_2 share only a single point $p = L_1 \cap L_2$ which is an end-point of each, then $\chi(L_1) + \chi(L_2) = \chi(L_1 \cup L_2) + \chi(p) = \chi(L_1 \cup L_2) + 1$, and since $L_1 \cup L_2$ is also a line segment (possibly not straight) homeomorphically equivalent to L_1 & L_2, one has $\chi(L_1 \cup L_2) = \chi(L_1) = \chi(L_2)$, whence it follows that χ for a line segment is $= 1$. Second, if two (non-straight) line segments L_1 & L_2 share two points each corresponding to end-points of L_1 & L_2, then one is similarly led to the conclusion that χ for a circle (here $L_1 \cup L_2$) is $= 0$. Third, for a disk one considers two "disks" D_1 & D_2 homeomorphically appearing as (filled-in) squares sharing a single edge $L = D_1 \cap D_2$, whence one has $\chi(D_1) + \chi(D_2) = \chi(D_1 \cup D_2) + \chi(L) = \chi(D_1 \cup D_2) + 1$, and since $D_1 \cup D_2$, D_1, & D_2 are homeomorphically each disks, one is also here led to $\chi(D) = 1$. To obtain χ for a sphere one considers two curved disks such that they share their full boundary in the form of a circle. For an open-ended cylinder one considers two square shaped disks which share opposite edges with one another: vertices a, b, c, d of the first square and a', b', c', d' of the second square are such that the (directed) line segment $a \to b$ of the first square corresponds to the (directed) line segment $a' \to b'$ for the second square, while similarly $c \to d$ corresponds to $c' \to d'$ – then one finds χ for an open-ended cylinder to be 0. If instead the two opposite-edge-sharing squares are chosen so that $a \to b$ & $a' \to b'$ correspond (as for the open-ended cylinder), while $c \to d$ corresponds to $d' \to c'$ (reverse to the case of an open ended cylinder), then one obtains χ for a Möbius strip as $= 0$. ■

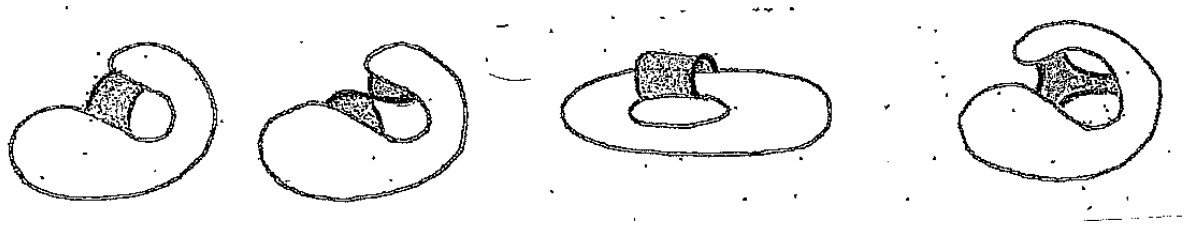

Figure 4. A surfacial structure S_0 with a shaded boundary-*p*-handle *D* added in different ways. In the first 3 figures $p = 1$ so that 2 disjoint portions of the boundary of *D* join to 2 disjoint portions of a boundary of S_0. The second case is of a Möbius-twisted 1-handle, and the last case has $p = 2$.

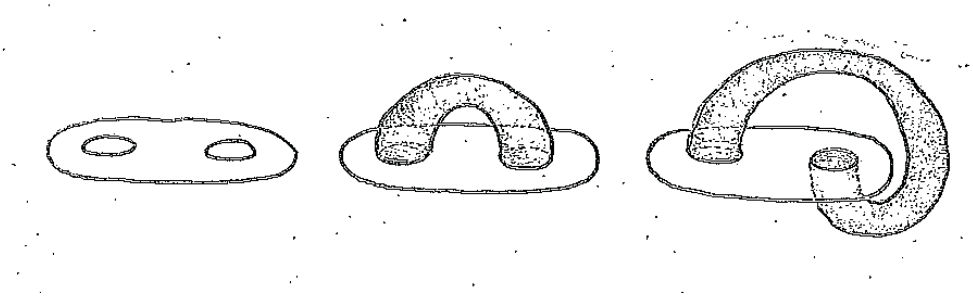

Figure 5. A doubly-punctured surfacial structure S_0 and then a tube-handle added in two different ways.

These results are well-known (in the general mathematical literature), with more examples in Ref. [26], but it seems of value to illustrate the use of the fundamental definition of (1), as proves of further use in the following.

A surface S_0 may be "decorated" in various ways. A *boundary*-p-*handle* adds to an S_0 with boundary by joining a "disk" *D* such that *D* shares exactly $p+1$ disjoint boundary line-segments with a like number of disjoint boundary line segment on S_0, as indicated in Figure 4. In general there are (topologically) different ways to make the gluing at the boundary or boundaries (as in Figure 4) which can change the "orientability" of the resultant surface, it being said that a surface is *orientable* if a (miniscule) walker on one side of the surface cannot get to the other side at the same point without crossing a boundary.

A *tube-handle* is added to *S* by taking an open-ended cylinder with both ends attached at the boundaries of 2 holes punched into *S*, as illustrated in Figure 5. This can be viewed as punching two holes in the parent surface and gluing the open-ends of the cylinder to the two holes.

Theorem 3 – Let S_{dec} be a "decorated" locally Euclidean surface which is obtained by adding to finite S_0 numbers $n_{\text{bdry-}p\text{-handle}}$ of boundary-*p*-handles, $n_{\text{tube-h}}$ of tube-handles, & n_{holes} of holes. Then

$$\chi(S_{\text{dec}}) = \chi(S_0) - n_{\text{holes}} - 2n_{\text{tube-h}} - \sum_p p \cdot n_{\text{bdry-}p\text{-handle}} \,.$$

Proof: This proceeds using the basic definition, after the fashion of the proof of the preceding theorem. Given a surface S_0 a first consideration is to punch a hole in S_0, thereby diminishing its χ-value by 1, as is seen upon considering the defining relation (1) along with $R = S_0 - \text{disk}$ & $T = \text{disk}$ with the two sharing just the circular boundary of *T*. That is, with each hole added χ is reduced by 1.

Next to add a *p*-handle, one considers S_0 and a "disk" *D* to share $p+1$ disjoint line segment boundaries. Then $S_0 \cap D$ consists of $p+1$ disjoint line segments. If $p = 1$, then $S_0 \cap D$ consists of 2 disjoint line segments, for which the definition of χ gives $\chi(S_0 \cap D) = 2$, whereupon $\chi(S_0) + \chi(D) = \chi(S_0 \cup D) + \chi(S_0 \cap D)$, which in turn gives $\chi(S_0) + 1 = \chi(S_0 \cup D) + 2$. For general $p \geq 1$, this argument is but slightly modified, with $S_0 \cap D$ consisting of $p+1$ disjoint line segments, for which one also readily sees that $\chi(S_0 \cap D) = p + 1$, and addition of a *p*-handle is seen to diminish the χ-value by *p*.

Next, for a tube-handle one considers appending an open-ended cylinder to a surface S_0, by first punching 2 holes in it and then taking an open-ended cylinder each of whose circular boundaries is to be glued to a corresponding boundary around a punched hole. The union of this double-punched surface (with χ diminished by 2 from the unpunched surface *S*) with the open-ended cylinder adds one handle, and again using the defining relation (1) one finds the result with the added tube-handle has the same χ-value as the double-punched surface. That is, with the addition of each tube-handle, the χ-value diminishes by 2. ■

Alternative proof: Let H_i, T_i and P_i be the *i* th hole, tube-handle and boundary-p-handle, then

$$\chi(S_{dec}) = \chi(S_0 \cup (\bigcup_{i=1}^{n_{holes}} H_i) \cup (\bigcup_{i=1}^{n_{t-h}} T_i) \cup (\bigcup_{i=1}^{n_{p-h}} P_i))$$

$$= \left\{ \begin{array}{l} \chi(S_0) + \chi(\bigcup_{i=1}^{n_{holes}} H_i) + \chi(\bigcup_{i=1}^{n_{t-h}} T_i) + \chi(\bigcup_{i=1}^{n_{p-h}} P_i) - \chi(S_0 \cap (\bigcup_{i=1}^{n_{holes}} H_i)) - \chi(S_0 \cap (\bigcup_{i=1}^{n_{t-h}} T_i)) - \\ \chi(S_0 \cap (\bigcup_{i=1}^{n_{p-h}} P_i)) - \chi((\bigcup_{i=1}^{n_{holes}} H_i) \cap (\bigcup_{i=1}^{n_{t-h}} T_i)) - \chi((\bigcup_{i=1}^{n_{holes}} H_i) \cap (\bigcup_{i=1}^{n_{p-h}} P_i)) - \chi((\bigcup_{i=1}^{n_{t-h}} T_i) \cap (\bigcup_{i=1}^{n_{p-h}} P_i)) \\ + \chi(S_0 \cap (\bigcup_{i=1}^{n_{holes}} H_i) \cap (\bigcup_{i=1}^{n_{t-h}} T_i)) + \chi(S_0 \cap (\bigcup_{i=1}^{n_{holes}} H_i) \cap (\bigcup_{i=1}^{n_{p-h}} P_i)) + \chi((\bigcup_{i=1}^{n_{holes}} H_i) \cap (\bigcup_{i=1}^{n_{t-h}} T_i) \cap (\bigcup_{i=1}^{n_{p-h}} P_i)) \\ - \chi(S_0 \cap (\bigcup_{i=1}^{n_{holes}} H_i) \cap (\bigcup_{i=1}^{n_{t-h}} T_i) \cap (\bigcup_{i=1}^{n_{p-h}} P_i)) \end{array} \right\}$$

Since $\chi(H_i) = 0$, $\chi(T_i) = 0$ and $\chi(P_i) = 1$ so we have

$$\chi(S_{dec}) = \left\{ \begin{array}{l} \chi(S_0) + 0 + 0 + n_{p-h} - n_{holes} - 2n_{tube-h} - n_{bdry-p-handle}(p+1) \\ -0 - 0 - 0 + 0 + 0 + 0 - 0 \end{array} \right\}$$

$$= \chi(S_0) - n_{holes} - 2n_{tube-h} - p \cdot n_{bdry-p-h}$$

Now if p is a variable i.e., $p = 1,2,3...$ and $n_{bdry-p-handle} = n_{bdry-1-handle}$, $n_{bdry-2-handle}$, $n_{bdry-3-handle}$, ..., then the above equation can easily be converted as

$$\chi(S_{dec}) = \chi(S_0) - n_{hole} - 2n_{tube-h} - \sum_p p \cdot n_{brdy-p-handle}$$ ■

When S is a surface without boundary (*i.e.*, is a surface closed in a geometric sense, which is to say a surface with no holes & no tube handles), this result is quite widely known, and then the number of tube-handles is termed the "genus" of S.

The Euler-Poincaré characteristic also relates to counts of further chemical substructures involving *cellular embeddings*, by which we mean a tiling covering S such that each tile is homeomorphic to a disk.

Theorem 4 – Let S be a locally Euclidean surface with a finite graph G cellular covering S such that G has $n = n(G)$ vertices, $e = e(G)$ edges, and $f = f(G \setminus S)$ faces (in its embedding). Then $n - e + f = \chi(S)$.

Proof: This can be established by induction, with the addition of faces 1 by 1. To initiate the induction, note that the relation is obviously fulfilled when there is a single face around a single "disk". This gives $\chi(D) = 1$ is a polygon (with $e = v \geq 3$). Now if a face is added to G_0 covering S_0 to give G covering S, we imagine that the face (a "disk") D shares some of its boundary with S_0. At this point the situation is viewed in terms of different cases depending on what D shares with S_0:

Case 1 – All D's boundary is shared with S_0. Then a hole is being filled, to increase the χ -value by 1, while G_0 & G are the same though we count 1 more face for its embedding, and granted the result for G_0, it follows for G.

Case 2 – Not all of the boundary of D is shared with S_0. Then this shared boundary consists of a number, say p, of disjoint "line segments", and the addition of D to S_0 corresponds to the addition of a p-handle to S_0 and thereby obtain S, whence $\chi(S) = \chi(S_0) - p$. But at the same time to obtain G from G_0, there are added alternating edges & sites between pairs of shared chains. With $p+1$ shared chains between G & G_0, there evidently are added also $p+1$ unshared chain sequences of edges joining pairs of shared chains. See an example in Figure 6. Any one of these unshared chain sequences contains 1 more edge than vertex, so that the difference $n - e$ diminishes by $p+1$ in going from S_0 to S. But also f increases by 1 in going from S_0 to S. Thus $n - e + f$ decreases by p.

And the induction is completed. ■

Alternative proof: Let for a pure polyhex, $S = \bigcup_{i=1}^{f} D_i$, where D_i is the disk of size i. Then

$$\chi(S) = \chi\left(\bigcup_{i=1}^{f} D_i\right) = \chi\left(\sum_{i=1}^{f} D_i\right) - \chi(\sum_{\forall i \neq j}^{f} D_i \cap D_j) + \chi(\sum_{\forall i \neq j \neq k \neq \ldots}^{f} D_i \cap D_j \cap D_k \ldots)$$

For polyhex the above expression would be

$$\chi(S) = \chi\left(\bigcup_{i=1}^{f} D_i\right) = \chi\left(\sum_{i=1}^{f} D_i\right) - \chi(\sum_{\forall i \neq j}^{f} D_i \cap D_j) + \chi(\sum_{\forall i \neq j \neq k}^{f} D_i \cap D_j \cap D_k)$$

$$= f - \chi(\sum_{\forall i \neq j}^{f} e_{ij}) + \chi(\sum_{\forall i \neq j \neq k}^{f} v_{ijk})$$

$$= f - e_{in} + v_{in}$$

Since $\chi(D) = 1$, $D_i \cap D_j = e_{ij}$, edges (i,j) and $D_i \cap D_j \cap D_k =$ a vertex where D_i, D_j and D_k meet, e_{in} and v_{in} are the number of internal edges and vertices respectively of the polyhex if it has a boundary. Let e_p and v_p are the number of edges and vertices on the boundary of the polyhex, then $e_p = v_p$ since boundary is a circuit. Thus $\chi(S) = f - (e_{in} + e_p) + (v_{in} + v_p) = f - e + v$.

If the polyhex does not have a boundary then $e_{in} + e_p = e_{in} = e$ and $v_{in} + v_p = v_{in} = v$.
Thus in general $\chi(S) = f - e + v$ holds. ■

The formula here is very well-known when S has no holes or p-handles (*i.e.*, S is without boundary) – especially in the circumstance when S is homeomorphic to a sphere. Note that here it was not even needed that G be pure-polyhex. If G is pure polyhex, and indeed is a benzenoid

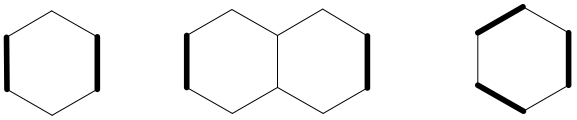

Figure 6. Example additions to form p-handles. The additions are imagined to be made by fusion at the bold-face bonds to an otherwise connected parent surface S_0. The first two cases here are for $p = 1$ -handles, and the third case is for a $p = 2$ -handle. In the first case when a 1-handle is being formed, the two S_0 -shared chains each contain a single edge, but the 2 unshared edge sequences shown in light-face involve internal vertices & not the end vertices: each sequence has 2 unshared edges & 1 unshared (internal) vertex for each sequence.

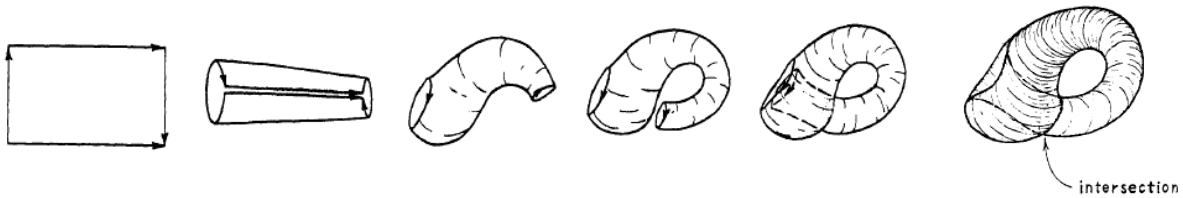

Figure 7. The step-by-step construction of a Klein bottle from a rectangular sheet ("disk"), with a self-intersection resulting between the 4th & 5th steps.

(with $\chi(S) = 1$) such that the area of each regular hexagonal face $= 1$, then the area occupied by G is $= f = e - n + 1$, as may be seen as a special case of Pick's theorem.[47,48] But this whole section is more general than the pure polyhex case – and is useful in the following.

CHARACTERIZATION OF PURE POLYHEX COVERINGS

First, there are some simple relations involving counts of various local sub-structures: $h(X)$ the number of hexagonal rings in X, $e(X)$ the number of edges in X, and $n_{\text{int}}(X)$ & $n(\delta X)$ the respective numbers of interior & boundary sites in X:

Theorem 5 – Let G be a finite pure polyhex species exactly covering a locally Euclidean surface S, whence the boundary δG of G coincides with the boundary δS of S. Then

$$n_{\text{int}}(G) = n(G) - n(\delta G)$$
$$2e(G) = 3n(G) - n_2(\delta G)$$
$$6h(G) = 3n(G) - n_\delta(G) - n_2(\delta G)$$

Proof: The first relation is particularly trivial, as $n(\delta G)$ & $n_{\text{int}}(G)$ are respectively the numbers of sites on & not on the boundary. The second relation is also readily obtainable, since $2e(G)$ counts the number of half bonds (or half edges), while this count also arises from $3n_3(G) + 2n_2(G)$, which in turn is just $3n(G) - n_2(\delta G)$. For the third relation, note that $6h(G)$ counts the number of interior angles (on the inside of face corners), as also clearly does $3n_{\text{int}}(G) + 2n_3(\delta G) + n_2(\delta G)$, which in turn is just $3n(G) - n(\delta G) - n_2(\delta G)$. ■

This result & proof exactly parallels that for benzenoids, for which these results are long (& well) known – see, *e.g.* Refs. [1,4,5].

Often a pure polyhex structure associates to a surface with boundaries. But not always:

Theorem 6 – Let G be a pure polyhex on a finite locally Euclidean surface S which has no boundary. If G is finite, then S is either a torus or a Klein bottle.

Figure 8. Interlacing mode in which an intersection of 2 parts of an original surface S can be circumvented through the introduction of strategically placed holes.

Proof: This has already been pointed out,[28] say by a relatively straight-forwardly approach, first utilizing theorems **4** and **5** to see that the surface S has $\chi(S) = 0$, and then looking at the mathematical literature to see just which boundaryless finite-area surfaces have $\chi(S) = 0$. ■

The case of a Klein bottle, indicated in Figure 7 (and named after Felix Klein[49]), necessarily entails self-intersections when embedded in 3-dimensional space, so that the associated polyhex structure is not chemically plausible. However, it may be pointed out that one could introduce a single large hole through which the tube is being pushed between the 4th & 5th panels of Figure **7**. Also if one were to use a Klein bottle with suitably placed "interlaced" holes, then self-intersections can be avoided, as indicated in Figure 8. It should be pointed out that an actual chemical bond does not fit well through the center of a small (say hexagonal) ring, so that these holes in Figure 7 are to have boundaries of length at least 10 edges, and perhaps desirably somewhat more.

The projective plane which again is nonorientable, may be obtained by adding a single *cross-cap* to a sphere as in Figure 9. Again the self-intersection can be avoided with the addition of suitably located holes, to make a structure which is in principal chemically realizable. Indeed a cross-cap implies non. But also it turns out that the sphere with cross-cap must have holes if it is to be tiled by hexagons. True cross-caps (without modification by adding such holes) are not the focus here. Indeed now we go on to surfaces with at least 1 boundary.

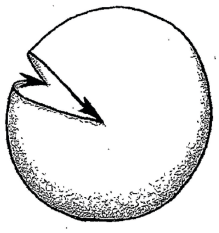

Figure 9. A cross-cap may be imagined, by first cutting a slice in a sphere opening it up a bit, orienting the edges as indicated above, then gluing the two sides of the slice back together again such that the arrows coincide, head with head, and tail with tail.

The different boundaries for finite-area S & G are crucial to the structures and may be characterized. For a connected component δ of the boundary, note that δ has no end, and so must be either infinite or a cycle from G. Now for our pure polyhex species every edge of δ occurs in a hexagonal ring of G, and the set of these hexagonal rings of G which share edges with δ form a subgraph G_δ. Often G_δ is a simple ordinary "bracelet" of fused hexagonal rings, but it need not be so – *e.g.*, G_δ could be a Möbius strip, possibly with a width of 1 hexagon, and possibly ≥ 2 hexagons width, or possibly of a width varying numbers of hexagons, or possibly G_δ can be a Möbius strip with 1 or more holes cut in it. In any event G_δ forms something which is broadly construable as a general *bracelet*, possibly with some number $t(\delta)$ of twists, associated with the manner in which its portion of surface S_δ is embedded in $\mathcal{E}_3$. See, *e.g.*, Figure 10. Formally given a strip S_δ in $\mathcal{E}_3$, first imagine a short (compared to non-neighbor hexagon separations) normal to the strip, tracing out a curve for the head of the normal as its tail circumscribes around the strip, and take $t(\delta)$ to be the minimum number of uncrossings of the tail and head curves needed to disentangle the two curves. That is, an ordinary bracelet has $t(\delta) = 0$, a Möbius strip has $t(\delta) = 1$, and higher numbers of twists are conceivable. If G_δ is of a single hexagon width, then whether $t(\delta)$ is odd or even is discernable, as this corresponds to whether there is 1 or 2 boundaries (comprised from the non-shared edges) of G_δ. Of course, if G_δ has an odd-parity $t(\delta)$, then the strip S_δ is *non-orientable* (in having only one side), whence also S is non-orientable. Presumably the greater the twist $t(\delta)$, the greater the stress in G_δ.

Lemma 7 – Let δ be a finite-length boundary of S_δ & S coverable by a pure polyhex graph G. Then δ is a cycle. If G_δ is *untwisted* (*i.e.*, $t(\delta) = 0$), then S_δ can be embedded in the plane all on one side of δ. If further G is finite, G_δ is either a benzenoid or has at least 2 boundaries.

Proof: That G_δ or the portion S_δ of S which is exactly covered by G_δ is untwisted means that S_δ can be homeomorphically embedded in the Euclidean plane $\mathcal{E}_2$ where the homeomorphism extends to the ambient space $\mathcal{E}_3$. A path δ_{center} from hexagon center to adjacent hexagon center also is topologically circular and does not cross δ, since δ being a closed curve in the plane, the Jordan curve theorem applies to say that δ divides the plane into 2 regions, an inside one and an outside one, with consequently δ_{center} on one side. The strip S_δ then has a second boundary outside of δ_{center}. ■

Figure 10. Three cyclic strips (or bracelets) with $t(\delta) = 0$, 1, or 2 twists.

A further boundary characteristic concerns the *mode of contact* of δ to a ring in G_δ, by which we mean a ring may make contact with 1, 2, or 3 successive strings of edges of δ, as illustrated in Figure 11. These different modes all occur with different benzenoids, but they can also occur on "internal" boundaries. In many cases G_δ is a bracelet with a width of a single hexagon, but not every hexagon of G_δ is incident to both the inner & outer boundaries, as indicated in Figure 12.

Beyond twisting there is also the possibility of *knotting*, by which we mean that we have a structure with some sort of handle such that it is embedded in Euclidean space $\mathcal{E}_3$ in such a way that it cannot be disentangled by a homeomorphism which also so maps the embedding space $\mathcal{E}_3$ as well. Neither this knotting nor the related topic of "linking" (involving graphically disconnected polyhex structures) are considered here. A subclass of such polyhexes of this sort is mentioned in Ref. [50] & more fully in Ref. [51] but is not pursued here.

The edges might be subcategorized, and counted. That is, let $e_{22}(\xi)$, $e_{23}(\xi)$, & $e_{33}(\xi)$ indicate numbers of

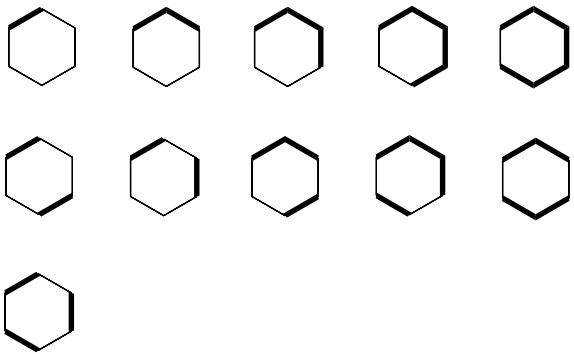

Figure 11. Singlet, doublet, & triplet modes of contact (between a ring & δ).

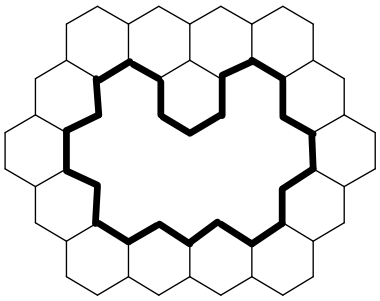

Figure 12. A strip graph G_δ for the boundary δ marked in bold face. A hexagon near the top of the bracelet is seen not to be incident with the outer boundary of G_δ.

edges for which their end vertices have the indicated degrees, (2,2), (2,3), or (3,3), as occur on the structure ξ, which could be a single boundary cycle, $\xi = \delta$, or the set $\xi = \partial G$ of all (disjoint) boundary cycles, or $\xi = \text{int}$ for the interior part of G, or the whole graph $\xi = G$. Then various relations apply with these quantities:

Lemma 8 – Let G be a finite-area pure polyhex. Then

$$2n_2(\delta) = 2e_{22}(\delta) + e_{23}(\delta)$$
$$2n_3(\delta) = 2e_{33}(\delta) + e_{23}(\delta)$$
$$n_3(\delta) \le 2e_{33}(\delta) \le 2n_3(\delta)$$
$$0 \le e_{23}(\delta) \le \min\{n_2(\delta), n_3(\delta)\}$$
$$0 \le e_{22}(\delta) \le n_2(\delta)$$
$$n_3(\partial G) + 3n(\text{int}) \le 2e_{33}(G) \le 3n_3(\partial G) + 3n(\text{int})$$

Proof: Most of these results are all based on counting half-edges, 2 half edges being associated to each edge counted by an e_{ab} and d half edges being attached to each such site being counted by n_d. Thus for the first equality, $2e_{22}(\delta) + e_{23}(\delta)$ counts half edges attached to a degree-2 site, as also does $2n_2(\delta)$. For the second equality, one counts δ's half edges attached to a degree-3 site – noting that though there are 3 half edges attached to a degree-3 site as counted by $n_3(\delta)$, only 2 of them are for each such site actually in δ. For the first (lower-bound) inequality of the third line, each edge of type (3,3) must have degree-3 sites on its ends each of which we can associate half of (as boundary sites) to that edge. For the second inequality of this third line (*i.e.*, for the upper-bound to $2e_{33}(\delta)$), one notes that no degree-3 site on the boundary δ may be associated to more than 2 edges of type (3,3) on δ. The lower-bound inequalities of the fourth & fifth lines are trivial. For the second inequality of the fourth line (i.e., the upper bound for $2e_{23}(\delta)$), one notes that each edge of type (2,3) must be associated with one degree-2 & degree-3 site on its 2 ends, so that there must be at least as many sites of each of these degrees on δG as there are type (2,3) edges. For the $2e_{22}(\delta)$ upper bound in the fifth line, note that no degree-2 vertex may be associated to more than 2 incident edges of type (2,2). In the sixth (& last) line, for the lower bound (to $2e_{33}(G)$), note that each interior site is of degree 3, so is attached to 3 half edges of type (3,3) occurring in the interior of G, and each degree-3 site in any boundary must be attached to 1 half edge also in the interior. Finally for the last inequality (the upper bound to $e_{33}(G)$), note that again each interior (degree-3) site is attached to 3 half edges, while each degree-3 site of ∂G can also be incident to no more than 3 such edges. ■

This lemma may be used in conjunction with Milan Randić's[52](renowned[53]) *connectivity index*

$$\gamma(G) \equiv \sum_{\{u,v\}}^{\in E(G)} \{d_u d_v\}^{-1/2} \qquad (2)$$

where d_u is the degree of site $u \in V(G)$. That is, upon noting that for pure polyhex graphs $\gamma(G) = \frac{1}{2}e_{22}(G) + \frac{1}{\sqrt{6}}e_{23}(G) + \frac{1}{3}e_{33}(G)$, we have bounds:

Corollary 9 – Let G be a finite-area pure polyhex graph. Then

$$\tfrac{1}{3}n_{3,G}(\partial G) + n_{\text{int}}(G) \le \gamma(G) \le n(G) + \sqrt{\tfrac{2}{3}} \cdot \min\{n_2(\partial G), n_3(\partial G)\}$$

The circumstance for benzenoids has already been considered.[54]

CURVATURE CHARACTERIZATION OF PURE POLYHEXES

Here the untwisted case is now the focus. As seen for benzenoids & multi-coronoids the difference between the numbers $n_2(\delta)$ & $n_3(\delta)$ of degree-2 & degree-3 vertices in a boundary component δ was important, and so it remains. To understand the significance, consider simple holes representing a ring of a size other than 6. In this case there are no sites of degree-2, and the result that $n_2(\delta) - n_3(\delta) = \pm 6$ of theorem 1 clearly does not hold for this δ. For this case, continued circumscription of ever larger bracelets of hexagons around the initial G_δ leads to a cone,[55] with the net Gaussian curvature in the region of the apex of the cone being $\{6 - n(\delta)\}\pi / 3$ – at least if the hexagonal rings in the surface of this cone are to remain not overly distorted. See, Figure 13. But this Gaussian curvature in the apex region is reflected[41,56] in circumscribing strips (for a more general untwisted G_δ) even well away from the apex. As a result it is natural to define

$$\kappa_G(\delta) = \{6 + n_2(\delta) - n_3(\delta)\}\pi / 3 \qquad (3)$$

as a *combinatorial curvature* associated to the boundary δ (or to the empty region adjoining δ). Note that for a boundary-δ hole in a coronoid (or multi-coronoid), one finds (*via* theorem **1**) that $\kappa_G(\delta) = 0$, which is to say that there is no "inherent" distortion by the sp^2-network

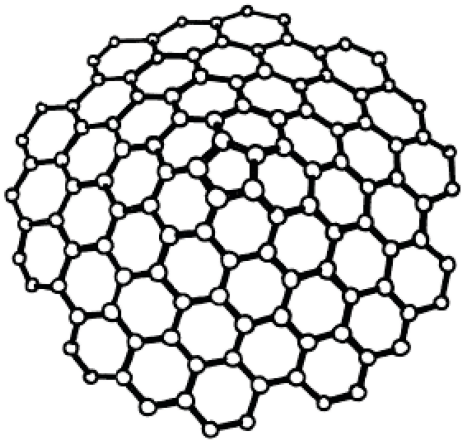

Figure 13. A pentagonal ring (identified with a hole in the complicit embedding surface *S*) surrounded by hexagons to form (perhaps just the beginning of) a cone.

skeleton to pull away from the flat case, with net integrated Gaussian curvature for a disk extended into the hole-region being $=0$. Another way to say this, is to identify $\kappa_G(\delta)$ to be the net combinatorial curvature of a planar graph fit into the hole region. Such a combinatorial curvature of a "filled-in" conjugated network is a fundamental graphic quantity, which is believed[25,26]to rather generally closely associate to (geometric) Gaussian curvatures. Moreover, exactly this definition has been utilized[57]to characterize untwisted "cyclo-polyphenacenes" (such as our untwisted G_δ is), and indeed κ_G for such a strip has even been found to correlate with stresses from *ab-initio* quantum-chemical computations.[58] That the combinatorial curvature for the outer boundary δ of a benzenoid (or regular multi-coronoid) G turns out to be $\kappa_G(\delta)=\{6+6\}\pi/3=4\pi$ is just saying that if such a (near planar) benzenoid were embedded on a sphere, it would preferably be very large sphere so that the hole region comprising the bulk of the sphere would manifest a net Gaussian curvature approaching that of the whole sphere (namely 4π). The difference in $n_2(\delta)-n_G(\delta)$ between inner & outer boundaries $\delta=\delta_{\text{in}}$ & $\delta=\delta_{\text{out}}$ for a multi-coronoid is 12 (in theorem 1), and is now seen to be but a reflection of the curvature difference between inner & outer open areas. Generally there is a coupling between curvature and occurrence of H atoms, which looks a little prettier if instead of measuring curvature in terms of radians (or ster-radians) one measures it in terms of full rotations,

$$\kappa_{\text{rot},G}(\delta)=\kappa_G/2\pi=1+\{n_2(\delta)-n_3(\delta)\}/6 \qquad (4)$$

That is, this takes simple rational values (in our circumstance, integral multiples of 1/6). The sum $6+n_3(\delta)-n_2(\delta)$ complicit here, and in theorem 1, simply measures combinatorial curvature in units of 60° turns. Then

Theorem 10 – Let *G* be a pure polyhex species, with a finite untwisted circuit boundary δ. Then $n_{\text{H}}(\delta)=3\kappa_{\text{rot,G}}(\delta)+\frac{1}{2}n(\delta)-3$. This curvature may be given in terms of the types of rings in *G*.

Proof: Of course the number of H atoms on δ is $n_2(\delta)$, and seeing that

$$n(\delta)+6\kappa_{\text{rot,G}}(\delta)=\{n_{2,G}(\delta)+n_3(\delta)\}+\{6+n_2(\delta)-n_3(\delta)\}=2n_2(\delta)+6,$$

one immediately obtains the claim. ■

This is of special significance if one understands the association between combinatorial curvature & Gaussian curvature for the realized molecular geometry. A formula for the curvature $\kappa_{\text{rot,G}}(\delta)$ can be given in rotations, if for the boundary graph G_δ (which we recall is a strip of hexagonal rings) we define for each ring α a *turn number* $t(\alpha)=-1, 0, 1, 2,$ or 3, as in Figure 14.

Theorem 11 – Let G be a pure polyhex species, with a finite untwisted circuit boundary δ & boundary graph G_δ. Then

$$\kappa_{\text{rot,G}}(\delta)=1+\frac{1}{6}\sum_{\alpha}^{\in G_\delta}t(\alpha).$$

Proof: Combinatorial curvature ($K_G(\delta)$) associated with the boundary can be written as

$$K_G(\delta)=[6+(n_2(\delta)-n_3(\delta))]\pi/3=2\pi+(n_2(\delta)-n_3(\delta))\pi/3.$$

Since there are 5 types of rings ($\alpha_i, i=1-5$) on a boundary graph G_δ as shown in Figure **14** and let α_i be the number of such types of ring with *i* (= 1 – 5) then above equation of $K_G(\delta)$ can be written as

$$K_G(\delta)=2\pi+\sum_{\alpha}^{\in G_\delta}\left[(i-1)-1\right]_\alpha\pi/3=$$

$$2\pi+\sum_{\alpha}^{\in G_\delta}\left[i-2\right]_\alpha\pi/3=2\pi+\sum_{\alpha}^{\in G_\delta}t(\alpha)\pi/3$$

Thus dividing both sides by 2π, we may obtain the theorem as

$$k_{rot,G}(\delta)=1+\frac{1}{6}\sum_{\alpha}^{\in G_\delta}t(\alpha)$$

where α runs over all rings in G_δ. ■

Theorem 12 – Let *G* be a finite-area pure polyhex on a surface *S* which in turn is topologically embeddable on a sphere. Then the net combinatorial curvature $\kappa(G)=\sum_\delta^{\partial M}\kappa(\delta)=4\pi$, and equivalently $\kappa_{\text{rot}}(G)=2$.

Proof: A straight-forward use of definitions gives the result:

$$\kappa(G)=\sum_\delta^{\partial M}\kappa(\delta)=(\pi/3)\sum_\delta^{\partial M}[6+(n_2(\delta)-n_{3G}(\delta))]=$$

$$[6+(n_2(\delta M)-n_3(\delta M))]\pi/3=4\pi$$

$$k_{rot,G}(\delta)=K(G)/2\pi=4\pi/2\pi=2.$$ ■

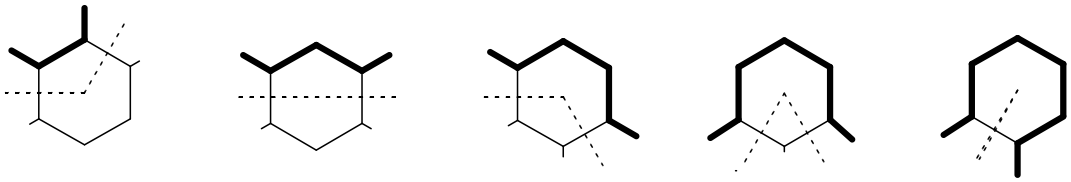

Figure 14. The 5 types of rings α on a boundary graph G_δ. The bold-face identifies the boundary δ, and the dotted line indicates the different angles of turn made, the turn number $t(\alpha)$ giving the turn at α in multiples of $\pi / 6$.

Here it should be noted that we do not necessarily concern ourselves with details of the embedding of S in $\mathcal{E}_3$. That is, even if a polyhex is embedded on a doubly twisted bracelet as in Figure 10, this so embedded S cannot be extended (retaining its embedding in $\mathcal{E}_3$) to something which is homeomorphic to a sphere in $\mathcal{E}_3$, it still can be homeo–morphically mapped into the 0-twist bracelet, which in turn is clearly homeomorphically embeddable on a sphere, so that the theorem still applies. This again provides a rationale as to why for multi-coronoids (as in theorem 1), the outer boundary gives $n_2(\delta) - n_3(\delta) = 6$ & the inner boundaries each gives $n_2(\delta) - n_3(\delta) = -6$: the outer boundary like that of a benzenoid gives a net curvature $= 4\pi$, while the inner boundaries give it $= 0$.

Another way to characterize a hole uses a boundary circuit δ. Imagine that the hole is filled in by a disk D_{hole} which shares the boundary δ, and further imagine that a graph G_{hole} is embedded on the disk such that it includes the boundary sites & edges of G, such that a new edge attaches to each one of the degree-2 sites (properly locating H atoms) on δ possibly with new degree-3 sites internal to D_{hole} so that G_{hole} divides D_{hole} into cells. Then this G_{hole} determines the combinatorial curvature of the hole:

Theorem 13: Let G be a pure polyhex species, with a finite untwisted circuit boundary δG, with a hole graph G_{hole}. Then $\kappa(G_{hole}) = (\pi / 3) \sum_{r_i}^{\in G_{hole}} (6 - i) \#_{r_i}(G_{hole})$, $\#_{r_i}$ is the number of hole r_i of size i in G_{hole}.

Proof: Since r_i s are the interior rings we may write

$$\kappa(G_{hole}) = \sum_{r_i}^{\in G_{hole}} \kappa^{(r_i)}(G_{hole}) = (\pi / 3) \sum_{r_i}^{\in G_{hole}} [6 \#_{r_i} - (n_3^{(r_i)} - n_2^{(r_i)}) \#_{r_i}]$$
$$= (\pi / 3) \sum_{r_i}^{\in G_{hole}} [6 - (n_3^{(r_i)} - n_2^{(r_i)})] \#_{r_i}$$

Now if the vertices on r_i are of degrees 3 and 2, $(n_{3G}^{(r_i)} - n_{2G}^{(r_i)}) = 6$ and such rings will not contribute to $\kappa(G_{hole})$ but if all vertices on r_i are of degree 3 then $(n_{3G}^{(r_i)} - n_{2G}^{(r_i)}) = n_{3G}^{(r_i)} = i$ and rings will contribute to $\kappa(G_{hole})$. Thus above equation can in general be written as

$$\kappa(G_{hole}) = (\pi / 3) \sum_{r_i}^{r_i \in G_{hole}} (6 - i) \#_{r_i}. \quad \blacksquare$$

Finally (for this section) we might list a summary tabulation of hole types in terms of G_{hole}, their combinatorial curvatures, and their proper H-atom counts.

Possible Types of Surfaces

The possible types of finite-area surfaces without boundary are already given in theorem **8**, so let us now proceed on to the case that the surface S has a single boundary.

Conjecture 14 – Let G be a finite pure polyhex on a surface S which has a single boundary δ. Then S is topologically a disk or a Möbius strip or generally an initially boundaryless surface with a hole. A hole would have $n_2(\delta) - n_3(\delta) = 6\chi(S)$ and integer curvature $\kappa_{\text{rot,G}}(\delta) = \chi(S)$.

Proof Attempt: Note that it has already been established that topologically (*i.e.*, up to homomorphism) there are only a select collection of finite-area surfaces with a single boundary, namely either a Möbius strip or a punctured finite-area surface or a disk. So let's proceed step by step, with a few cases.

Let us begin with the Möbius strip can be tiled with hexagons – an ordinary cyclic belt of hexagons may be cut (across the belt), twisted once, and then reconnected. Indeed there are very many ways to tile a Möbius strip with hexagons.

Next, we imagine that we start with a surface S_0 having no boundary, and then introduce a hole into it to obtain S. Then the Euler characteristics of S & S_0 are related (*via* theorem **3**) as $\chi(S) = \chi(S_0) - 1$. Now from theorem **8** and the result that $n(G) = n_{\text{int}}(G) + n_2(\delta G) + n_3(\delta G)$, $e(G) = \frac{3}{2} n(G) - \frac{1}{2} n_2(\delta G)$, and $h(G) = \frac{1}{2} n(G) - \frac{1}{6} n(\delta G) - \frac{1}{6} n_2(\delta G)$, from which via theorem **5**, we obtain $\chi(S) = \{n_2(\delta G) - n_3(\delta G)\} / 6$. Thus $\chi(S_0) = 1 + \{n_{2,G}(\delta) - n_{3,G}(\delta)\} / 6$, so that since $\chi(S_0)$ is integer, and ≤ 2, one has that $n_{2,G}(\delta) - n_{3,G}(\delta) = 6, 0, -6, -12, \ldots$. The case, that $n_{2,G}(\delta) - n_{3,G}(\delta) = 6$ corresponds to S_0 being a sphere and S being a disk, which is to say that G is (topologically) an

ordinary benzenoid. The case $n_{2,G}(\delta) - n_{3,G}(\delta) = 0$ corresponds to S_0 with $\chi(S_0) = 1$, which means that it is a sphere with a cross-cap and S is a disk with a cross-cap. That such an S might support a hexagonal tiling is suggested in Figure 15, for a graph with 18 vertices, 18 + 6 edges, & 3+2 hex-rings. This gives an Euler characteristic $\chi = 18 - 24 + 5 = 1$, so that we might imagine this corresponds to our cross-capped case. Such constructions can start from larger annulenes, say of 30 sites.

Proceeding for the case where $n_{2,G}(\delta) - n_{3,G}(\delta) = -6$, this evidently corresponds to S_0 with $\chi(S_0) = 0$, so that S_0 is (via theorem **6**) either a Klein bottle or a torus – and it is clear that either of these surfaces when punctured can support a hexagonal tiling – by just removing a connected collection of tiles & associated surface fragment from an otherwise hexagonally tiled surface. For $n_{2,G}(\delta) - n_{3,G}(\delta) \leq -12$, the corresponding S_0 have $\chi(S_0) \leq -1$, and these do not have hexagonal tilings. But puncturing such surfaces to give S can result in something that is hexagonally tilable. In Figure 16, we illustrate such a construction: first, starting from g tori, each of which is tilable by hexagons (Figure 16); second, puncturing each by removal of a connected set of hexagons; and third, joining them by additional hexagons in such a way that a single boundary surface S results, which if the hole is filled in by surface (without worrying about tiling) yields a genus-g surface S_0 with $\chi(S) = 2 - 2g$. The illustration in Figure 16 is just for $g = 1,2,3$, but it is clearly extendable – and though the basic tori illustrated are all the same, they need not be. Indeed, any one of the tori can be replaced by a Klein bottle – just put the hole in the half of a Klein bottle which looks like half of a torus. Indeed, one may use a sphere with a cross cap, even though such a surface is not hexagonally tilable – the surface obtained in the second stage, where a hole is punched in the sphere (to give a disk with a cross-cap) is tilable by hexagons. Thus one finds the requisite examples of surfaces S with arbitrary negative (integer) $\chi(S)$. ■

Chemo-physical studies of cases with a single boundary other than the classical benzenoids are somewhat limited, though there are examples. For instance, Möbius

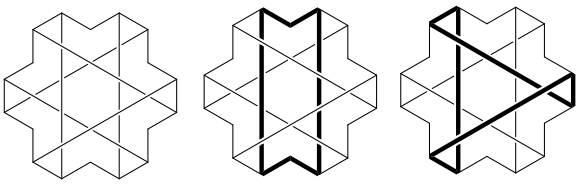

Figure 15. An 18-site annulene with 6 additional long-bonds added in (a) in the first row, to give a result with 3 hex-rings of the bold-face type in (b), and 2 hex-rings of the bold-face type in (c).

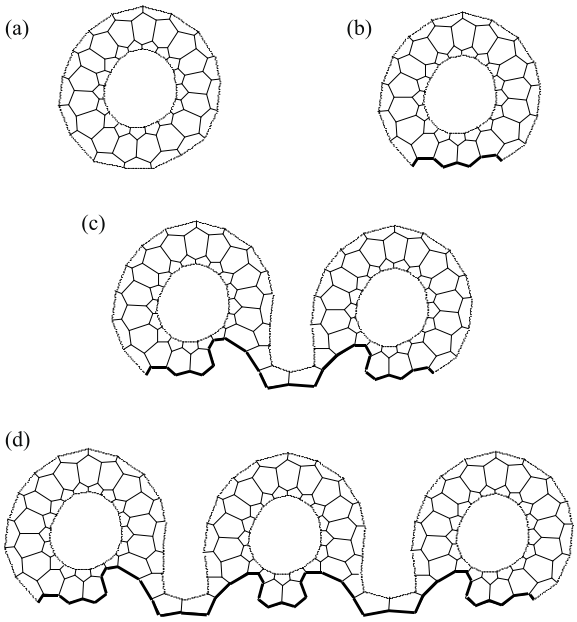

Figure 16. Surfaces with lower Euler characteristic showing the possibility of hexagonal tilings. In (a) a torus covered by hexagons is indicated, where just half of the tiled surface is shown – the dotted lines are not edges, but rather just a marking of the division between the front half & back half of the torus (and a front & back half of a hexagonal face) and only half-edges are incident at these dotted lines. In (b) a hole is introduced with its boundary (on the shown half) indicated in bold-face. In (c) two of the punctured tori of (b) are interconnected by a strip of hexagons, and in (d) three of the punctured tori are joined – in both (c) & (d) only a single cyclic boundary remains, again with its front half shown in bold-face.

twisted polyacenes also have been studied,[59–63] as well as the more general case of a Möbius-twisted poly-phenacenes, still of 1-hexagon width. Indeed wider strips have also been studied.[64,65] The case of a single-boundary structures with $\chi(S) < 0$, seem not to have been contemplated comprehensively before. Our case of Figure 15 with 18 sites & $\chi(S) = -1$ surely seems to have excessive steric strain. But there are more plausible looking cases with the same topology (but more sites) – as in Figure 17, for a topologically equivalent structure with 42 sites. A more geometric view takes 2 hexagons a bit apart normal to a common axis, with 3 anthracene chains, each of which with ends fused to alternating sides of the 2 axial hexagons. Yet also, these anthracene interconnections are each Möbius twisted – the result has just a single boundary, reminiscent of an ordinary Möbius band. It looks a bit like an American football, excepting the 3 Möbius twists. The structure also looks similar to the "catacondensed chemical hexagonal complexes" of Anstöter *et al.*[66]

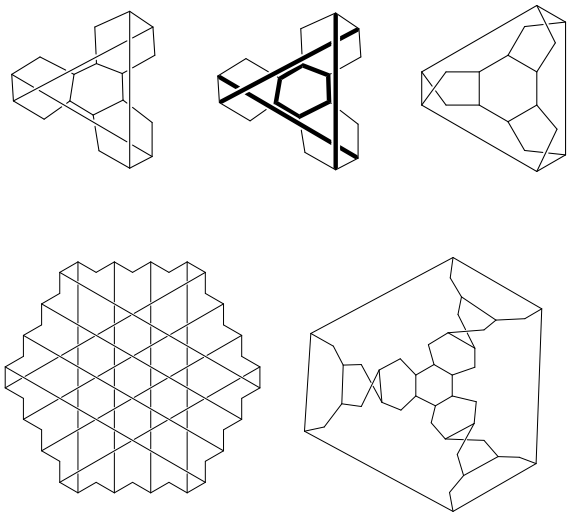

Figure 17. In the first row a redrawing of the structure of Figure 15. In the second row a structure with the same topology but with 42 sites rather than just 18. Also it has 11 hexagons, 3 of which are "Möbius twisted"

Pure polyhex surfaces corresponding to $\chi(S) \leq -2$ do not correspond to any hexagonally tilable closed surface S_0 obtained by filling in the hole with additional surface – because of conjecture **14**, but also as seen in the present conditions on $n_{2,G}(\delta) - n_{3,G}(\delta)$, there are no suitable hexagonal tilings for the added surface filling in the hole (as this difference takes a different value than is required by theorem **1**). That is, if the hole is filled in by additional π-network, it would need to involve a topological "defect" (making it other than a pure polyhex, such as addressed here).

Theorem 15 – Let *G* be an infinite pure polyhex on a surface *S* which has no boundary. Then *S* is $\mathcal{E}_2$ or an infinite cylinder or a semi-infinite cylinder capped by a cross-cap.

Proof: Obviously the result is true for $\mathcal{E}_2$ where *G* is just the honeycomb lattice. To deal with surfaces *S* which have some kind of "defect", we note that one could cut out a hexagon tiled region including the "defect" to obtain a surface S_0 as in the attempted proof for conjecture **14**. Thus to determine such *S*, we proceed *via* an examination of the finite-area hexagon-tilable surfaces S_0 with a single boundary and check to see which can be extended *via* repeated circumscription of hexagons to an infinite graph. ■

The case of an infinite pure polyhex on a surface *S* with a single boundary is also of interest. If the boundary is finite, this evidently includes *S* as a punctured plane $\mathcal{E}_2$ corresponding to graphene with some faces removed. But this choice for *S* also includes nano-cones and dislocations – *e.g.*, as described in.[22,41,58] Still with a finite boundary, there is a possibility of a infinite cylinder (or tube) either with an open end or with a hole. For the infinite cylinder with a hole, the hole may be made by simply removing some hexagonal faces, but also there is a possibility of a hole like a dislocation, in which case the tube is of different "types" on each side of the dislocation, and also there is the possibility that it be like a disclination of negative curvature, in which case it opens up like a funnel. If both *G* & its boundary are infinite, then *S* can evidently be a half-plane.

Here it might be commented that the case that *S* is a half-plane involves rather different sorts of possibilities which might be distinguished via a refinement of the notion of homeomorphism. Let $d(x,y)$ & $d'(x',y')$ denote distances between pairs of points in two surfaces *S* & *S'*. Let *S* & *S'* each support polyhex graphs *G* & *G'* such that the near-regular hexagons in both *S* & *S'* are of very nearly the same size. Then *S* & *S'* are *boundedly* homeomorphic if there is a homeomorphism $\varphi : S \to S'$ such that there exists a finite $D \in \mathbb{R}$ for which $\left| d(x,y) - d'(\varphi x, \varphi y) \right| \leq D$ for all points $x, y \in S$. Now, for example, all finite benzenoids are boundedly homeomorphic, because we did not specify a value for *D* except to say that it was finite. But maybe this puts different homeomorphic surfaces into different classes, such as is considered below.

Next imagine that from the regular honeycomb network (*i.e.*, graphene) in $\mathcal{E}_2$ one obtains *sectors* via cuts from the center of a central hexagon straight outward through centers of surrounding hexagons. Further define an *m*-sector to consist of *m* such sectors with the i^{th} joined to the $(i+1)$ th just as in the honeycomb network, $i \in [m-1]$, and $m = 1,2,3,4,\ldots$. The "degenerate" 0-sector is defined to be a semi-infinite strip of hexagons. Each of these *m*-sectors is imagined to consist of very nearly regular hexagons with the surface *S* into which it is embedded having vanishingly small curvatures. Perfect regularity & perfect planarity is achievable for $m = 0,1,2,3,4,5$, all within $\mathcal{E}_2$, and the central angle on *S* where the *m* different sectors meet is $\vartheta_m = m\pi / 3$. But for $m \geq 6$ one needs to have a sort of helicenic structure – somewhat as with multiple Riemann sheets spiraling around the origin.

Theorem 16 – Granted this sectioning of graphene & rejoining, each of *m*-sectors, $m = 0,1,2,3,4,\ldots$, is in a distinct class of boundedly homeomorphic surfaces.

Proof: It is clear that each of these *m*-sectors S_m is homeomorphic to the ordinary half-plane (which is essentially S_3). So an initial point concerns whether any pair of them are boundedly homeomorphic. For an *m*-sector made from near regular hexagons with a near-planar surface, one obtains central angles $\vartheta_m \cong m\pi / 3$. Then for a homeomorphism $\varphi : S_m \to S_{m'}$, one sees that the boundedly homeomorphic condition implies that equally spaced points (say the graph vertices) on the two boundary segments directed away from the central apex of S_m would

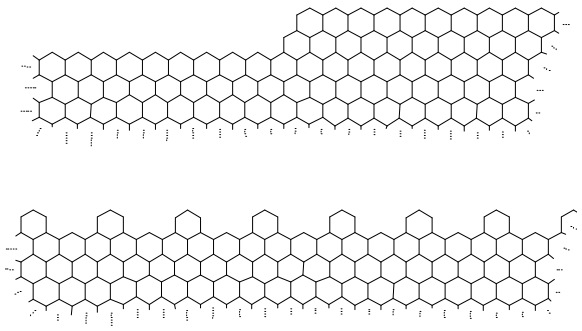

Figure 18. Indications of two infinite boundaries. The first has a single region where there is a step up in what is otherwise a "straight" zig-zag boundary. The second boundary is translationally symmetric, and can be viewed as periodically adding additional rings to the 3-sector.

need to end up being nearly equally spaced (to within a distance D) in the mapping to S_3. Indeed consider similar rays of points directed away from the central apex nearly along each of the additional "boundaries" of the component 1-sectors combined together to form S_m. Evidently if the points within any a first boundary ray (say on the "left") and the next one in (at 60° from this "left" boundary) are to satisfy the boundedly homeomorphic condition this second ray of points would under the mapping φ end up being radially directed outward from the apex in $S_{m'}$, and ultimately at large distances ($>> D$) from the apex be directed nearly radially outward from the apex of $S_{m'}$ & at ultimately at very nearly an angle of 60° from the "left" boundary ray of $S_{m'}$. One could continue until finally one obtains a ray that does not match the boundedly homeomorphic condition to the "right" boundary of $S_{m'}$. That is, the different m-sectors are not boundedly homeomorphic to one another. ■

A further question is whether there are any other polyhex tilable surfaces with a single infinite boundary. All these are imagined to be simply homeomorphic to the half-plane – and preclude an infinite-length Möbius strip, which is not thought to make "sense". Let us comment on different pure polyhexes which are nevertheless boundedly homeomorphic. Two such examples are indicated in Figure 18, each of which is boundedly homeomorphic to S_3. In the first "stepped" example of Figure 18, one can imagine fusing a couple 0-sectors to a 3-sector, and there is a homeomorphism which takes the i^{th} boundary ring of this first example to the i^{th} boundary ring of S_3, and similarly on into the interior. Thence one sees that boundaries that such a "notched" boundary involving the addition of say d 0-sectors each with the ends of the 0-sectors close by ends up being boundedly homeomorphic with $D \sim d$. In the second translationally symmetric example in Figure 18, there are additional hexagons periodically attached to S_3. In such an example, one can imagine a homeomorphism φ in which each additional ring α along with the rings to which α is attached are mapped to these corresponding attachment rings in S_3, and otherwise the other rings are mapped to corresponding rings in S_3. Thence such a φ describes a bounded homeomorphism with D roughly the size of such an attachment region. We speculate that the different boundedly homeomorphism classes for all surfaces simply homeomorphic to the half-plane might correspond to "pie-shaped" sections of the honeycomb net with different angles ϑ from a central apex.

PROGNOSES & CONCLUSIONS

It is seen that there is a diverse class of "pure polyhex" molecular π-network structures, for possible use in various nano-devices. For these structures there are non-trivial combinatorial structure-counting relations & conditions related to the topological & geometrical features of these structures. These relations extend standard results for the special case of benzenoids, as well as some fullerenes, and a few other special cases previously studied. Here unified and extended interpretations & consequences are found, particularly in terms of combinatorial curvatures, which are believed to correlate with geometric Gaussian curvatures, and consequent geometric realizations. The results here provide further support that combinatorial curvature is a fundamental concept – helping to characterize, and understand, various possible structures. Steps are taken toward the identification of all possible types of topological surfaces which are hexagonally tilable, most especially for the case that there are either 0 or 1 boundaries to the surface. The case of no boundaries, gives rise to just a finite number of topological possibilities: (infinite) graphene, infinite nanotubes, & bucky-tori – and the nanotubes and nano-tori can be knotted. Our demand of embedding of the polyhex into a 2-dimensional manifold S which in turn is embedded into Euclidean 3-space excludes the possibility of polyhex-tiled Klein bottles (as the related S intersects itself). The case of a single boundary has been attempted to be treated in a somewhat comprehensive way, though even here leading to an infinite number of topological cases – aside from the further possibility of knotting of the boundary in Euclidean 3-space.

There has been much work with special cases of two boundaries, for instance, the case of coronoids has long been extensively contemplated (as reviewed elsewhere[18]). Also different bracelet-like structures have been addressed, *e.g,* with work on cyclo-polyacenes going back some time,[32] and many more recent studies, represented by the Refs. [67–70] Most such cases considered entail holes with 0 combinatorial curvature, though there has been consideration[56,57] with this

curvature being non-zero. For 2 or more boundaries, the topological possibilities seem to become truly bewildering. Nevertheless some of our results still apply.

A further question concerns schemes by which to encode boundaries δ, such as we have found to be so important in understanding the possible purely polyhex structures. Recalling that vertex degrees d_u $(=2$ or 3), $u \in V(G)$, a *boundary code* $\mathfrak{c}(\delta)$ for δ could be defined as the sequence of values $c_u(\delta) \equiv d_u - 2$ for the different vertices u when one proceeds along δ with the bulk of the polyhex on the right. Of course there are different starting points, and one might choose a starting point lexicographically: the sequence of digits of $\mathfrak{c}(\delta)$ is to be a smallest such binary number. One might have entertained also choosing the direction around δ to minimize this number (just as has been proposed[71] for benzenoids, and benzenoid polymers) – but the choice to keep the bulk of the polyhex (*i.e.*, G_δ) on the right helps ascertain relative orientations of any different boundaries. Now, $\sum_u^\delta c_u(\delta) = n_3(\delta)$ & $\sum_u^\delta \{1 - c_u(\delta)\} = n_2(\delta)$, while $\sum_u^g \{2c_u(\delta) - 1\}$ is our net turn number. But really the boundary code is more to specify the shapes of the boundaries – and could be a subject of future consideration.

In dealing with nano-structures, one often wishes to deal with infinite polyhexes, say as a reference. Some of our theorems require the polyhex structure to be finite, but theorems **3**, **6**, & **7** do not (though some of these are only about finite boundaries – e.g., of holes in a buckytube, or graphene strip, or even a full sheet of graphene).

Another point concerns structures of a more general class, say which does not have any hexagonal faces (such as polyenes) or even if they do have hexagons, edges not in a hexagon are allowed (such as biphenyl). The given condition of local Euclideanicity would presumably be relaxed, to allow "strings" to be attached to our current sort of surface. This could be a subject of future development. A sort of theoretical development somewhat parallel to what we have done here might be made, deleting these strings (of edges not in any hexagon) and investigating the remnant pure polyhex network. Some (and perhaps much) of the commentary on combinatorial curvature would remain intact, but the identification of degree-2 sites with H atoms would need to be modified (to allow either H atoms or "strings" to be there. This also is left for later. Though a diverse range of structures are here illuminated, it seems that there remains much more to do, as concerns geometric structure, but especially as concerns electronic structure. Even general results for the last item involving the simple Hückel model (involving adjacency-matrix eigen-spectra) and resonance theory (involving perfect or near-perfect matchings) should be of interest. The strength and stability of the bonds formed in these polyhex species, indicates a high potential for use in nano-science. We see the study of pure polyhexes as but barely begun, though there has been extensive work on numerous subclasses, by numerous numbers of researchers.

Here we would like to mention three prominent such researchers (who are chemical graph theoreticians): Dr. Prof. Milan Randić, Dr. Ed Kirby, and Prof. Mircea Diudea (each of whom at least one of us count as close friends). We dedicate this work to them. Notably there many more chemical graph theoreticians long active in this area: N. Trinajstić, A. T. Balaban, I. Gutman, H. Hosoya, S. J. Cyvin, J. R. Dias, W. C. Herndon, as well as several close colleagues, and undoubtedly several more whom we have not mentioned. Even further this general area (of benzenoids & beyond) has received much attention, with our current effort being to open up the field a bit more in a general mathematical framework.

Acknowledgment. Support (via grant BD-0894) from the Welch Foundation of Houston, Texas, is gratefully acknowledged.

REFERENCES

[1] I. Gutman, *Croat. Chem. Acta* **1974**, *46*, 209–215.
[2] J. R. Dias, *J. Chem. Inf. Comp. Sci.* **1982**, *22*, 15–22. https://doi.org/10.1021/ci00033a004
[3] J. R. Dias, *Acc. Chem. Res.* **1985**, *18*, 241–248. https://doi.org/10.1021/ar00116a003
[4] S. J. Cyvin, I. Gutman, *Kekulé Structures in Benzenoid Hydrocarbons*, Springer Verlag, Berlin, **1986**.
[5] I. Gutman and S. J. Cyvin, *Introduction to the Theory of Benzenoid Hydrocarbons*, Springer Verlag, Berlin, **1990**. https://doi.org/10.1007/3-540-51505-4
[6] S. J. Cyvin, *J. Math. Chem.* **1992**, *9*, 389–391. https://doi.org/10.1007/BF01166103
[7] J. Brunvoll, B. N. Cyvin, S. J. Cyvin, *J. Chem. Inf. Compl. Sci.* **1994**, *34*, 903–911. https://doi.org/10.1021/ci00020a026
[8] J. R. Dias, *MATCH Commun. Math. Comput. Chem.* **1983**, *14*, 83–138.
[9] J. R. Dias, *Chem. Phys. Lett.* **1991**, *185*, 10–15. https://doi.org/10.1016/0009-2614(91)80131-G
[10] J. Brunvoll, B. N. Cyvin, S. J. Cyvin, *Zeit. Naturforschung* **1993**, *48a*, 1017–1025. https://doi.org/10.1515/zna-1993-1010
[11] S. J. Cyvin, B. N. Cyvin, J. Brunvoll, *J. molec. Struc.* **1993**, *300*, 9–22. https://doi.org/10.1016/0022-2860(93)87003-R
[12] S. J. Cyvin, B. N. Cyvin, J. Brunvoll, *Chem. Phys. Lett.* **1995**, *240*, 601–604. https://doi.org/10.1016/0009-2614(95)00568-O

[13] S. J. Cyvin, B. N. Cyvin, J. Brunvoll, E. K. Lloyd, *Disc. Appl. Math.* **1996**, *67*, 67–78. https://doi.org/10.1016/0166-218X(95)00011-F

[14] B. N. Cyvin, J. Bruvoll, S. J. Cyvin, *MATCH Commun. Math. Comput. Chem.* **1996**, **33**, 35–46.

[15] J. R. Dias, *Adv. Molec. Similarity* **1998**, *2*, 257–262.

[16] M. Deza, P. W. Fowler, V. Grishukhin, *J. Chem. Comp. Sci.* **2001**, *41*, 300–308. https://doi.org/10.1021/ci000060o

[17] M. D. Sikirić, M. Deza, M. Shtogrin, *Disc. Appl. Math.* **2008**, *156*, 1518–1535. https://doi.org/10.1016/j.dam.2006.11.020

[18] a) S. J. Cyvin, J. Brunvoll, B. N. Cyvin, *Theory of Coronoid Hydrocarbons*, Springer Verlag, Berlin, **1991**. b) S. J. Cyvin, J. Brunvoll, R. S. Chen, B. N. Cyvin, F. J. Zhang, *Theory of Coronoid Hydrocarbons II*, Springer Verlag, Berlin, **1994**. https://doi.org/10.1007/978-3-642-51110-3

[19] T. G. Schmalz, W. A. Seitz, D. J. Klein, G. E. Hite, *J. Am. Chem. Soc.* **1988**, *110*, 1113–1127. https://doi.org/10.1021/ja00212a020

[20] P. W. Fowler, D. E. Manolopoulos, *An Atlas of Fullerenes*, Oxford University Press, Oxford, **1995**.

[21] M. Deza, P. W. Fowler, A. Rassat, K. M. Rogers, *J. Chem. Inf. Comp. Sci.* **2000**, *40*, 550–558. https://doi.org/10.1021/ci990066h

[22] W. F. Harris in *Fundamental Aspects of Dislocation Theory* (Eds.: J. A. Simmons, R. de Wit, R. Bullough), US NBS Pub. #317, Washington, DC, **1970**, pp. 579–592

[23] J. P. Gaspard, R. Mosseri, J. F. Sadoc, *Phil. Mag. B* **1984**, *50*, 557–567. https://doi.org/10.1080/13642818408238878

[24] J.-F. Sadoc, R. Mosseri, *Geometrical Frustration*, Cambridge University Press, Cambridge, **1999**. https://doi.org/10.1017/CBO9780511599934

[25] D. J. Klein, X. Liu, *Intl. J. Quantum Chem. S* **1994**, *28*, 501–523. https://doi.org/10.1002/qua.560520845

[26] D. J. Klein, H. Zhu, *All-Conjugated Carbon Species* in *From Chemical Topology to Three-Dimensional Geometry* (Ed.: A. T. Balaban), Plenum Press, New York, **1997**, pp. 297–341. https://doi.org/10.1007/0-306-46907-3_9

[27] E. C. Kirby, *Croat. Chem. Acta* **1993**, *66*, 13–26.

[28] D. J. Klein, *J. Chem. Inf. Comp. Sci.* **1994**, *34*, 453–459. https://doi.org/10.1021/ci00018a037

[29] E. C. Kirby, R. B. Mallion, P. Pollak, *J. Chem. Soc. Faraday Trans.* **1993**, *89*, 1945–1953. https://doi.org/10.1039/ft9938901945

[30] S. Itoh, S. Ihara, J. Kitakami, *Phys. Rev. B* **1992**, *47*, 12908–12911. https://doi.org/10.1103/PhysRevB.47.12908

[31] D. Babić, D. J. Klein, T. G. Schmalz, *J. Mol. Graphics Modell.* **2001**, *19*, 223–231. https://doi.org/10.1016/S1093-3263(00)00115-7

[32] E. Heilbronner, *Helv. Chim. Acta* **1954**, *37*, 921–935. https://doi.org/10.1002/hlca.19540370336

[33] D.J. Klein, W.A. Seitz, T.G. Schmalz, *J. Phys. Chem.* **1993**, *97*, 1231–1236. https://doi.org/10.1021/j100108a020

[34] O. Ivanciuc, L. Bytautas, D. J. Klein, *J. Chem. Phys.* **2002**, *116*, 4736–4748. https://doi.org/10.1063/1.1450547

[35] D. Hilbert, S. Cohn-Vossen, *Anshauliche Geometrie of 1932* translated to English in *Geometry and the Imagination*, Chelsea, New York, **1952**. https://doi.org/10.1007/978-3-662-36685-1

[36] J. L. Kelley, *General Topology*, D. Van Nostrand Pub., New York, **1955**.

[37] M. Henle, *A Combinatorial Introduction to Topology*, W. H. Freeman, San Francisco, **1979**; Dover, **1994** (reprint).

[38] J. Stillwell, *Classical Topology and Combinatorial Group Theory*, Springer Verlag, Berlin, **1990**.

[39] M. Terrones, F.Banhart, N. Grobert, J. C. Charlier, H. Terrones, P. M. Ajayan, *Phys. Rev. Lett.* **2002**, *89*, 075505. https://doi.org/10.1103/PhysRevLett.89.075505

[40] R. Lv, E. Cruz-Silva, M. Terrones, *ACS Nano* **2014**, *85*, 4061–4069. https://doi.org/10.1021/nn502426c

[41] D. J. Klein, *Phys. Chem. – Chem. Phys.* **2002**, *4*, 2099–2110. https://doi.org/10.1039/b110618j

[42] *Molecular Catenanes, Rotaxanes, & Knots* (Eds.: J.-P. Sauvage, C. Dietrich-Buchecker), Wiley-VCH, NYC, **1999**.

[43] H. Hadwiger, *Elem. Math.* **1947**, *2*, 127.

[44] H. Hadwiger, J. Reine, *Angew. Math.* **1955**, *194*, 101–110. https://doi.org/10.1515/crll.1955.194.101

[45] V. Klee, *Am. Math. Mon.* **1963**, *70*, 119. https://doi.org/10.2307/2312880

[46] Y. A. Shashkin, *The Euler Characteristic*, MIR Pub., Moscow, **1989**. (translated from a Russian publication of **1984**).

[47] G. Pick, *Sitzungsber. Lotos Prague* **1900**, *19*, 311–319.

[48] D. E. Varberg, *Am. Math. Mon.* **1985**, *92*, 584–587. https://doi.org/10.1080/00029890.1985.11971689

[49] F. Klein, *Uber Riemans Theorie der Algebraischen Funktionen und Ihre Integrale*, Teubner, Leipzig, **1882**. (an English translation was published by Dover in **1963**).

[50] D. J. Klein, A. Misra, *MATCH Commun. Math. Comput. Chem.* **2002**, *46*, 45–69.

[51] W. Yang, F. Zhang, D. J. Klein, *J. Math. Chem.* **2010**, *47*, 457–476. https://doi.org/10.1007/s10910-009-9583-8

[52] M. Randić, *J. Am. Chem. Soc.* **1975**, *97*, 6609–6615. https://doi.org/10.1021/ja00856a001
[53] L. B. Kier, L. H. Hall, *Molecular Connectivity in Chemistry and Drug Research*, Academic Press: New York, **1976**.
[54] R. Pepper, D. J. Klein, *MATCH Commun. Math. Comput. Chem.* **2007**, *58*, 359–364.
[55] A. T. Balaban, D. J. Klein, X. Liu, *Carbon* **1994**, *32*, 357–359. https://doi.org/10.1016/0008-6223(94)90203-8
[56] D. J. Klein, A. T. Balaban, *J. Chem. Inf. Mod.* **2006**, *46*, 307–320. https://doi.org/10.1021/ci0503356
[57] A. Misra, D. J. Klein, *J. Chem. Inf. Comp. Sci.* **2002**, *42*, 1171–1175. https://doi.org/10.1021/ci020030g
[58] J. Cz. Dobrowolski, *J. Chem. Inf. Comput. Sci.* **2002**, *42*, 490–499. https://doi.org/10.1021/ci0100853
[59] J. F. Krebs, R. W. Zoellner, *Proc. Natl. Couf. Undergrad. Res.* **1991**, *5*, 652–657.
[60] L. Türker. *J. Molec. Struct.* (*Theochem*) **1998**, *454*, 83–86. https://doi.org/10.1016/S0166-1280(98)00232-2
[61] E. W. S. Caetano, V. N. Freire, S. G. dos Santos, D. S. Galvão, F. Sato, *J. Chem. Phys.* **2008**, *128*, 164719. https://doi.org/10.1063/1.2908739
[62] E. M. Olmedo, S. Fomine, *Russian J. Phys. Chem.* **2019**, *93*, 723–729. https://doi.org/10.1134/S0036024419040216
[63] E. Sadurní, F. Leyvraz, T. Stegmann, T. Seligman, D. J. Klein, *J. Math. Phys.* **2021**, *62*, 052102. https://doi.org/10.1063/5.0031586
[64] K. Wakabayashi, K. Harigaya, *J. Phys. Japan* **2003**, *22*, 998–1001. https://doi.org/10.1143/JPSJ.72.998
[65] K. Harigaya, A. Yamahiro, Y. Shimoi, K. Wakabayashi, Synth. *Metals* **2005**, *152*, 261–264. https://doi.org/10.1016/j.synthmet.2005.07.093
[66] C. S. Anstöter, S. N. Bašić, P. W. Fowler, T. Pisanski, *Croat. Chem. Acta.* **2020**, *93*, (online first). https://doi.org/10.5562/cca3765
[67] G. Dorflinger, H. Sofer, *Monatsch. Chem.* **1969**, *99*, 1866–1875. https://doi.org/10.1007/BF00904320
[68] G. Ege, H. Vogler, *Theor. Chim. Acta* **1974**, *35*, 189–202. https://doi.org/10.1007/BF00546904
[69] S. Kivelson, O. L. Chapman, *Phys. Rev. B* **1983**, *28*, 7326. https://doi.org/10.1103/PhysRevB.28.7236
[70] F. J. Zhang, S. J. Cyvin, B. N. Cyvin, *Monastsch. Chem.* **1990**, *121*, 421–432. https://doi.org/10.1007/BF00809459
[71] D. J. Klein, W. C. Herndon, M. Randić, *New J. Chem.* **1988**, *12*, 71–76. https://doi.org/10.1002/cc.36819886411